

Carpal hyperextension in Nigerian Dwarf goats is a heritable syndrome associated with lameness and forelimb deformity

Leah Streb, DVM, MPH¹; Erica McKenzie, BVMS, PhD, DACVIM^{2*}; Carrie Finno, DVM, PhD, DACVIM¹; Susanne Stieger-Vanegas, DVM, PhD, DECVDI²; Christiane Löhner, VetMed, Dr med vet, PhD, DACVP² ; Rachael Gruenwald, DVM, DACVP²; Constance White, DVM, PhD²

¹School of Veterinary Medicine, University of California-Davis, Davis, CA

²College of Veterinary Medicine, Carlson College of Veterinary Medicine, Oregon State University, Corvallis, OR

*Corresponding author: Dr. McKenzie (erica.mckenzie@oregonstate.edu)

Objective

To characterize an acquired carpal hyperextension syndrome reported by North American owners of Nigerian Dwarf goats and examine potential genetic associations.

Methods

Affected (cases) and unaffected (controls) Nigerian Dwarf goats were recruited into this observational study from 2022 to 2023 through a small ruminant producer email list and social media. Animals with reported limb trauma, cases with mild carpal angulation, and controls under 2 years old were excluded. Physical examination, carpal goniometry and blood mineral analysis were performed on all animals. Husbandry and registration information were recorded by a standardized questionnaire. Imaging and histopathology were performed on a subset of cases. Pedigrees were analyzed for common ancestor(s) with Pedigraph. A genome-wide association study was performed with the Illumina GoatSNP50 array.

Results

36 cases (carpal angle > 187°) and 64 controls were included. Owners recognized cases at a median age of 12 months (IQR, 12 to 24 months; range, 3 to 36 months); lameness was common in cases. Median standing carpal angle of cases when bearing weight was 193.3° (IQR, 190.2° to 198.3°) versus 180.3° in controls (IQR, 180.0° to 180.7°). Imaging and histopathology did not identify a structural cause. Blood mineral concentrations were similar between groups. Pedigree analysis indicated all cases shared a single ancestor. Genome-wide analysis identified a region of interest (chr24:59,830,666-60,251,280) associated with the hyperextension phenotype.

Conclusions

Carpal hyperextension in Nigerian Dwarf goats was often associated with lameness and appears heritable.

Clinical Relevance

Small ruminant producers and veterinarians should be alert to this potentially heritable condition. Carpal goniometry of standing animals represents an inexpensive and minimally invasive diagnostic procedure.

Keywords: hyperextension, goniometry, goat, pedigree, MRI

The Nigerian Dwarf goat (NDG) is a US-developed dairy goat breed commonly used for milk and cheese production, showing, and youth agricultural projects. Nigerian Dwarf goats share common West African origins with the American Pygmy breed.¹ Though multiple national and international goat registries now accept the NDG, the breed was initially established by the American Goat Society, with 2,000 foundation animals accrued from 1984 to 1997, after which the herdbook was closed.¹ The

breed has increased in popularity as a dairy breed, and currently a large number of NDGs are registered with the American Dairy Goat Association (ADGA).² The ADGA registered more than 28,000 new NDGs in the year 2024, accounting for nearly half of all new caprine registrations.³ The breed is now a well-recognized and popular choice throughout the US but draws its origins from a fairly narrow genetic lineage, increasing the risk for hereditary disease occurrence.

Over approximately the last 15 years, a syndrome of acquired carpal hyperextension has been described by NDG owners and is anecdotally reported to be increasing in incidence. The condition is characterized by progressive hyperextension of one or both carpal joints, often before 2 years of age, frequently with concomitant lameness. Owners have

Received December 15, 2025

Accepted February 4, 2026

Published online March 18, 2026

doi.org/10.2460/javma.25.12.0790

©The authors

reported that affected goats within their herds are often related, suggesting potential heritability. The disorder carries welfare and financial implications for animals and their caregivers and producers, with increased veterinary expense and constraint of show and production value. Since this syndrome may not be recognized in a timely manner and bucks reach sexual maturity before 1 year of age, affected males may sire many offspring prior to identification of carpal hyperextension. Since NDG females tend to have large litter sizes, affected does may also have multiple offspring before phenotype recognition.

The purpose of this study was to (1) develop a description of the clinical and pathological characteristics of carpal hyperextension in NDGs for use as a preliminary basis for diagnostic classification with carpal goniometry, imaging, and histopathology and (2) determine heritability of this syndrome and candidate genomic regions by use of pedigree and genome-wide association analyses, respectively. We also aimed to explore any contribution of management factors such as housing, ration, and use to development of carpal hyperextension via a standardized questionnaire and evaluation of blood mineral concentrations.

Methods

Nigerian Dwarf goats were recruited for the study from August 2022 to February 2023 through a small ruminant producer email list and a preexisting social media site (the Carpal Hyperextension in Nigerian Dwarf Goats Facebook page⁴). All animals were privately owned and examined either at the Oregon State University Lois Bates Acheson Veterinary Teaching Hospital or during on-site farm visits conducted by the investigators in Oregon and Washington. This study was approved by the IACUC at Oregon State University (IACUC-2021-0239), and owners of all included animals reviewed and signed a consent form describing the study prior to animal enrollment.

Inclusion criteria for all animals were the following: the animal was of the NDG breed, and either the individual or both dam and sire were ADGA registered. Candidate cases were selected based on owner-identified visible hyperextension of the carpus, at any age. Hyperextension cases identified by owners were then confirmed on examination by consensus of 2 investigators (LS, EM). Up to 2 control animals/case were selected from farms contributing cases, with preference given to selection of controls that were related to cases (full or half siblings or parents). To avoid misclassification of disease status, we selected control animals that were at least 2 years of age and that owners perceived had no evidence of carpal deformity, which was subsequently confirmed by the investigators. Goats with any known history of limb trauma were excluded from the study.

Bilateral forelimb ultrasound and radiography were performed on a subset of affected goats. A number of these imaged animals were donated due to severity of lameness associated with carpal hyperextension. Donated animals were humanely euthanized by IV overdose of barbiturate solution, after which post-mortem MRI of the forelimbs, followed by complete necropsy and histopathology, was performed.

A standardized questionnaire was used to collect relevant information for each enrolled goat. Information was collected in regard to signalment, housing, use, medical history, ration and supplements, ADGA registration number, parentage, and caprine arthritis and encephalitis virus (CAE) test status. In affected goats, additional information was collected to characterize the history of their carpal hyperextension, including age of onset, limb(s) affected, changes in carpal deformity over time, and any diagnostic procedures or treatments performed.

All goats were weighed on the same digital scale provided by investigators at the time of examination and scored for body condition score by 1 of 2 investigators (LS, EM) with a 5-point system.⁵ Lameness was evaluated with animals at rest in a standing position and during a 20-m in-hand walk and graded with a modified 4-point Sprecher scale.⁶ Goniometry was performed on both carpi of all goats by use of landmarks previously described in dogs (**Figure 1**).^{7,8} Distance between forelimb distal phalanges at the tips of the claws during voluntary standing position was also measured to quantify toe splay. All measurements were obtained with goats standing on a hard, flat surface. A single investigator (LS) performed all measurements on all goats to limit interobserver variability, under supervision of a second investigator (EM) for consensus. Measurements for each limb were taken in triplicate to generate an average carpal joint angle for each evaluated limb.

Forelimb radiography was performed on both front limbs of 11 affected goats in a standing position with both front feet positioned on top of 8-cm-high wooden blocks. One goat required a small amount of sedation (xylazine; 0.02 mg/kg, IM) to facilitate the procedure. Lateral, dorsopalmar, dorsolateral-palmaromedial oblique, dorsomedial-palmarolateral oblique, and flexed lateral views were obtained on both front limbs from the mid antebrachium distally, including the digits. Ultrasound of both forelimbs from the distal antebrachium to the second phalanx was performed on a subset ($n = 8$) of the radiographed goats with a MyLab SigmaVET (Esaote SpA) equipped with a linear transducer (4-15 MHz; Esaote SpA). Magnetic resonance imaging (Signa Horizon 1-T MRI; GE HealthCare) of the forelimbs was performed immediately after death on these 8 animals (6 were imaged bilaterally and 2 unilaterally on their affected limb), with bodies left intact to facilitate positioning. Imaging from distal antebrachium to proximal aspect of the proximal phalanx was performed in the following sequences: (1) a T1-weighted sequence (echo time, 14.9 milliseconds; repetition time, 566.6 milliseconds; flip angle, 90°; slice thickness, 2 mm; interslice gap, 0.5 mm) acquired in transverse, frontal, and sagittal planes; (2) a T2 fast spin echo sequence (echo time, 93.18 milliseconds; repetition time, 6,616.7 milliseconds; flip angle, 90°; slice thickness, 2 mm; interslice gap, 0.5 mm) acquired sagittally; and (3) a proton-density fast spin echo sequence (echo time, 44 milliseconds; repetition time, 2,000 milliseconds; flip angle, 90°; slice thickness, 2.5 mm; interslice gap, 0.5 mm) acquired in transverse and frontal planes. All imaging was performed and interpreted by the same board-certified veterinary

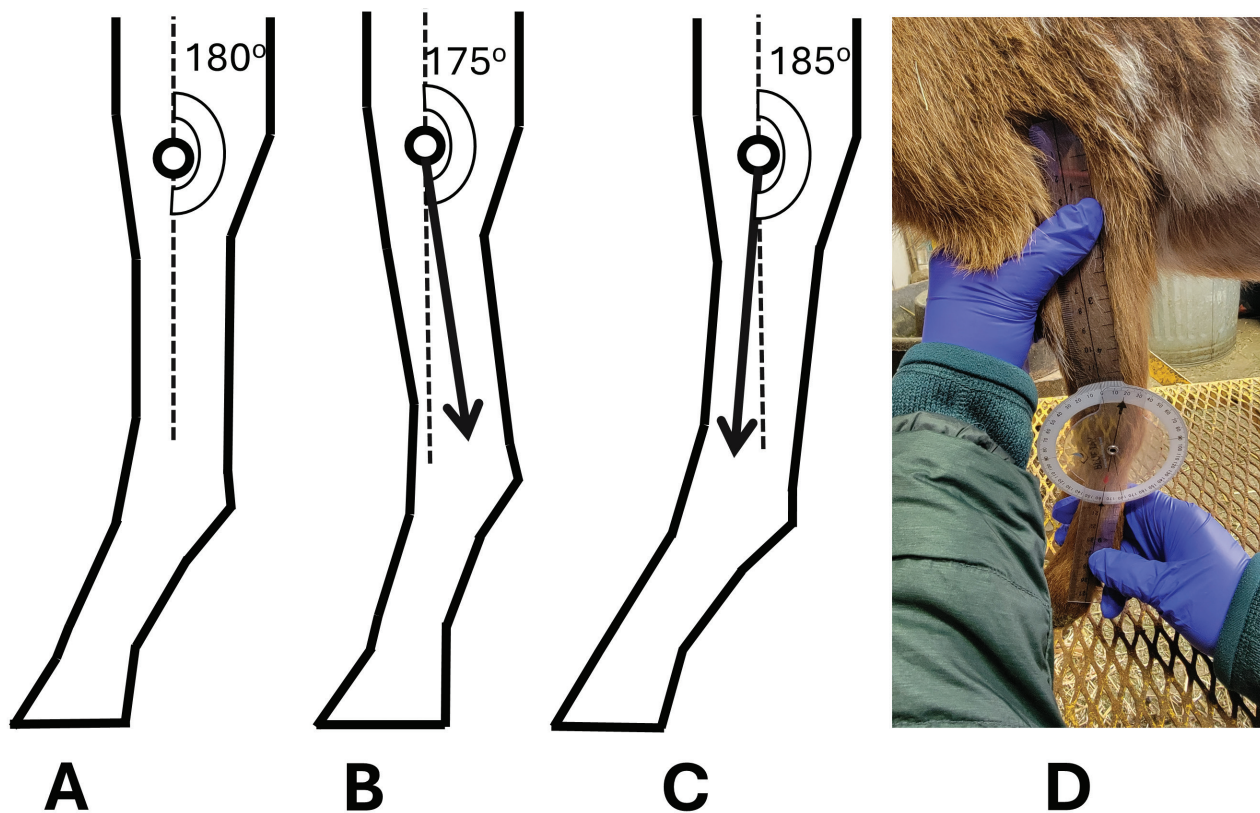


Figure 1—Carpal goniometry. The center of the goniometer is placed over the axis of joint rotation. The proximal goniometer arm is placed against the lateral humeral epicondyle, and the distal goniometer arm is placed along the lateral metacarpus long axis, aligned with the palpable lateral prominence at the distal metacarpus. A—Carpal angle at 180°. B—Carpus in mild flexion (< 180°). C—Carpus in mild hyperextension (> 180°). D—Carpal goniometry being performed on an affected goat.

radiologist (SSV; European College of Veterinary Diagnostic Imaging diplomate).

Whole blood was collected into EDTA for DNA extraction. Samples were refrigerated until DNA extraction, which was performed within 5 days of collection. The DNA was extracted according to manufacturer recommendations (Gentra Puregene Blood Kit; Qiagen), resuspended in Tris-EDTA, and stored at -80 °C. Serum or sodium heparinized plasma was also collected from all animals at the time of evaluation. Supernatants were stored at -80 °C and subsequently submitted to Texas A&M Veterinary Medical Diagnostic Laboratory for analysis of cobalt, copper, iron, manganese, molybdenum, selenium, and zinc concentrations by inductively coupled plasma mass spectrometry.

Necropsy and histopathology were performed and interpreted by a single board-certified pathologist (CL; American College of Veterinary Pathologists diplomate) on a total of 10 of the imaged goats. Carpal joints were sectioned sagittally to capture the radiocarpal joint, intercarpal joint, and carpometacarpal joint, with joint capsule and ligaments. Superficial and deep digital flexor tendons and associated muscles were collected separately. Routine necropsy samples (**Supplementary Table S1**) were also collected and prepared with standard techniques.

Pedigrees were assembled from the breed registry database (ADGA Genetics⁹), farm/breeder websites,

and Pedigree Online.¹⁰ A minimum of 5 to 7 generations were collected where records were available. Pedigree¹¹ was used to create pedigrees and allow for the visualization of affected animals and common relatives.

Genotyping was performed with the Illumina Goat-SNP50 Beadchip genotyping array at Neogen Corp (Lansing, Michigan). This array contains 53,347 single-nucleotide polymorphisms (SNPs), which were mapped with the goat assembly ARS1.2 (2016; GenBank accession GCA_001704415.2). Single-nucleotide polymorphism data cleaning and quality control were performed with Plink (version 1.9; Christopher Chang, Carson Chow, Shashaank Vattikuti, et al).¹² Individuals missing more than 10% of genotypes were excluded from analysis. Single-nucleotide polymorphisms with a minor allele frequency < 5% or genotyping call rate < 90% were excluded from analysis. Single-nucleotide polymorphism association analysis used a standard case-control design. Genomic inflation (λ) was calculated with Plink.¹² Manhattan and quantile-quantile plots were generated with qqman¹³ and MultiMeta¹⁴ packages in RStudio (version 2025.05; Posit Software PBC). A Bonferroni correction was used to adjust the critical α threshold for statistical significance at $P_{\text{Bonferroni}} < .05$. Suggestive significance was set at a false discovery rate of 10%. Regions of interest around SNPs identified in genomic analysis were screened for candidate genes with the goat genome assembly ARS1.2 (2016).

Statistical analysis

Stata/BE (version 19; StataCorp LLC) was used for nongenomic statistical analysis. Continuous data were assessed for normality with the Shapiro-Wilk test; descriptive statistics are reported as median, interquartile interval, and range for any data that were not normally distributed. Statistical tests of group differences in continuous data were performed with the Mann-Whitney *U* (Wilcoxon rank sum) test or independent sample *t* test, depending on normality. Associations between management or demographic factors were examined with univariate logistic regression and/or exact logistic regression, depending on cell counts. Critical α for statistical significance was set at $< .05$, with Bonferroni correction for multiple comparisons.

Results

Clinical characteristics

A total of 105 goats from 17 farm sites were recruited for enrollment in the study. *Controls* were classified as animals with a standing carpal angle of $< 184^\circ$. *Cases* were defined as goats with a standing carpal angle $> 187^\circ$. To ensure a strict phenotype, animals with standing carpal angles between 184° and 187° on either limb ($n = 5$) were excluded, leaving 36 cases and 64 controls for the purposes of analysis.

Cases and controls were similarly aged at the time of initial examination and similar in body weight, body condition score, and height (Tables 1 and 2).

Table 1—Clinical characteristics of affected (cases) and unaffected (controls) goats.

	Affected goats	Unaffected goats	<i>P</i> value*
Males	15 (42%)	9 (14%)	.0022
Females	21 (58%)	55 (86%)	—
Unilaterally affected	18 ($n^{**} = 36$)	—	—
Bilaterally affected	18 ($n^{**} = 36$)	—	—

*Univariate logistic regression for categorical variables. **Number of animals with information recorded. — = Not applicable.

Table 2—Additional clinical characteristics of affected (cases) and unaffected (controls) goats

	Affected goats				Unaffected goats				<i>P</i> value*
	Median	IQR	Range	<i>n</i> **	Median	IQR	Range	<i>n</i> **	
Age (y) at examination	3.95	2.47–4.62	1.22–8.74	36	3.64	2.76–6.14	1.33–11.89	64	.1174
Body weight (lb)	72.5	54.4–90	29.1–116	34	75.0	64.5–87	43–108	64	.5705
Body condition score	3	2–3	1–5	33	3	2.5–3.5	1–5	61	.0979
Height (inches)	21.25	20–22.75	17.5–25.75	32	20.55	19.75–21.5	17.25–26	62	.2627
Standing carpal angle ($^\circ$)	193.3	190.2–198.3	187.3–201.3	36	180.3	180.0–180.7	178.7–183.3	64	.0000
Males only	193.3	190.7–198.7	189.3–200	15	180.3	180–180.7	180.0–181	9	.0000
Females only	193.0	190.0–197.3	187.3–201.3	21	180.3	180–180.7	178.7–183.3	55	.0001
Age (mo) at which condition noticed	12	12–24	3–36	30	—	—	—	—	—
Lameness score	2	1–2	0–3	27	0	0–0	0–2	60	.0000

*Mann-Whitney *U* (Wilcoxon rank sum) for continuous variables; univariate logistic regression for categorical variables. **Number of animals with information recorded. — = Not applicable.

A greater proportion of affected animals were male, compared to controls. Median weightbearing carpal angle was 193.3° in cases and 180.3° in control animals (Figure 2).

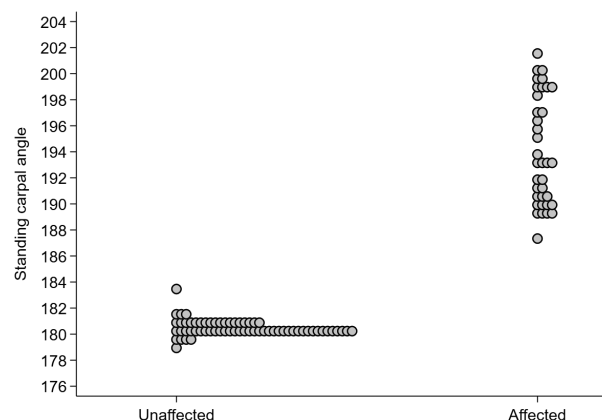


Figure 2—Dot plot of standing carpal angles in unaffected (controls) and affected goats (cases). Each circle represents 1 individual animal.

Half of all cases were bilaterally affected. Owners recognized carpal hyperextension in the affected goats at a median age of 12 months. In all but 1 case, limb changes were noticed at or after 6 months of age (Supplementary Figure S1). Most affected animals in which gait could be evaluated were lame (14 of 27 had grade 2 lameness, 11 of 27 had grade 1 lameness, and 5 of 27 had no lameness observed). In contrast to carpal angles, toe splay was not different between cases and controls (Supplementary Table S2).

Cases and controls were reported to be similarly managed, with no significant differences evident in feeding or supplement practices between the groups (Supplementary Table S3). A higher proportion of controls were used for breeding and/or dairy production. A higher proportion of control animals were tested for CAE infection, though no positive results were reported in either group. Animals that were not tested for CAE were reported to come from closed herds. No significant differences were detected in serum or plasma trace mineral concentrations between the 2 groups (Supplementary Table S4).

Previous veterinary care for carpal deformity was recorded for 13 affected goats; administration

of systemic NSAIDs, nutritional supplements, and laser therapy were reported as treatments in 1 or more cases. A total of 18 affected goats had been removed from breeding programs by their owners after they recognized carpal hyperextension.

Imaging

A total of 22 forelimbs from 11 affected goats were radiographed. The majority of carpi had 1 or more radiographic signs of degenerative joint disease (periarticular osteophytes, $n = 5$; enthesophytes, 6; remodeled distal radius, 3), as well as radiocarpal joint subluxation (3) and widened radiocarpal joint space (5; **Figure 3**). Bilateral forelimb ultrasound was performed



Figure 3—Dorsopalmar and lateromedial radiographs of the right (A and B) and left (C and D) carpus to distal phalanges of a 2-year-old buck with severe bilateral carpal hyperextension with bilateral moderate radiocarpal degenerative joint disease and moderate right and severe left enthesiopathy along the medial aspect of the radiocarpal joint. There is bilateral mild palmar subluxation of the radiocarpal joint.

in 8 of these 11 animals. Ultrasound abnormalities were found in the forelimbs of 3 animals, while the remaining 5 were unremarkable. On ultrasound, one animal had mild right fetlock joint effusion and bilateral distal flexor tendon sheath effusion with no anomalies of the tendons. Another had mild extracapsular thickening of both carpi with arthritic changes, and the third had a small amount of anechoic fluid adjacent to the distal aspect of the right lateral oblique sesamoidean ligament. On MRI images of the tendons and ligaments of 14 legs of 8 affected goats (2 imaged only unilaterally, on their 1 affected leg), no abnormalities of the flexor or extensor tendons or of the collateral ligaments of the carpus and metacarpophalangeal joint were found. In 1 animal, there was mild thickening bilaterally of the extracapsular soft tissues along the dorsal aspect of the carpi, worse dorsomedially and mildly heterogeneously hyperintense in signal intensity.

Gross and histopathologic examinations

Eight of the imaged goats (16 forelimbs) underwent gross and histopathologic examinations after humane euthanasia. Gross carpal lesions consisted of expansion of 1 or more carpal synovial sacs (carpi, $n = 3$), synovial thickening (carpi, 2), and visibly evident cartilage thinning (carpi, 2). On histopathologic examination, all carpal joints had some degenerative changes; specifically, articular cartilage erosion (carpi, $n = 12$), ulcerated and/or necrotic cartilage (carpi, 6), and synovial hyperplasia (carpi, 10). No lymphocytic/plasmacytic infiltrate was observed in any joint. One 2-year-old buck showed small amounts of retained cartilage in the metaphyseal spongiosa in both legs. Multiple nonmusculoskeletal gross and histologic findings were also present in examined animals (**Supplementary Table S5**).

Pedigree analysis

Over 20 generations were traced back with available records and mapped with Pedigraph. All affected animals included in this study were traced back to a single common ancestor (**Supplementary Figure S2**).

Genome-wide association analysis

A total of 94 animals were genotyped, 5 of which failed sample quality control at Neogen. Two additional goats were genotyped; however, neither met the case criteria and were excluded from the analysis (one had an intermediate carpal angle and another, initially classified as a control, was reported by the owner to have developed carpal hyperextension after our evaluation). These goats were therefore labeled as *unknown* and not included in the analysis. After quality control of SNPs in Plink, 47,297 SNPs remained and 33 cases and 54 controls had been genotyped at $> 90\%$ and were therefore analyzed. The PLINK-calculated genomic inflation factor was $\lambda = 1.06$, suggesting minimal population stratification. However, the quantile-quantile plot from the genome-wide association suggested that the study was underpowered (**Figure 4**).

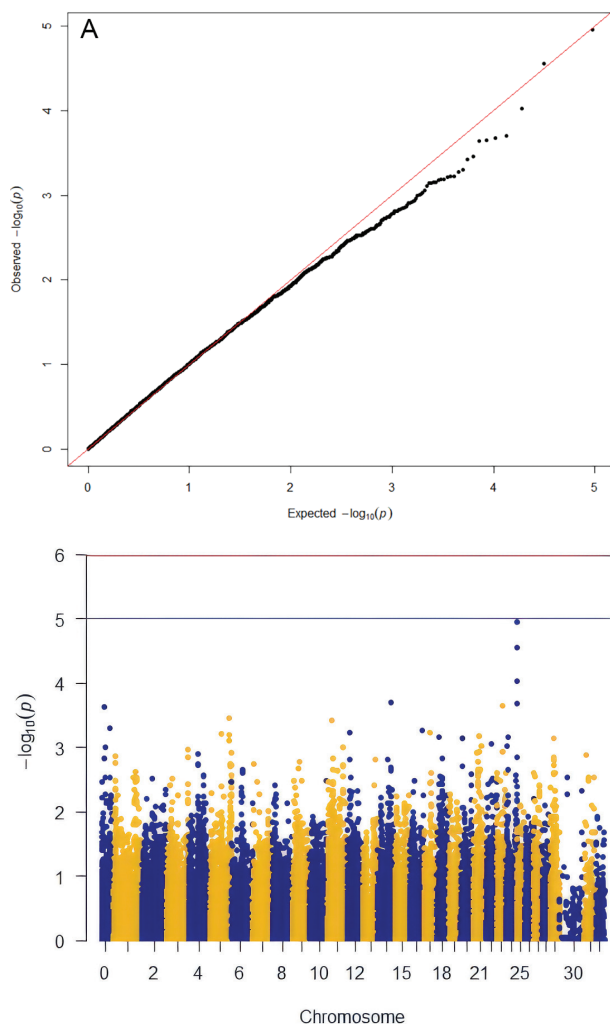


Figure 4—A—Quantile-quantile plot from the genome-wide association study of genotyped animals ($n = 87$). P values under the diagonal line suggest the study is underpowered. B—Manhattan plot from the genome-wide association study of genotyped animals ($n = 87$). The red line denotes Bonferroni significance, and the blue line denotes 10% false discovery rate correction. One single-nucleotide polymorphism achieved suggestive significance (chr24:59830666, $P = 1.10 \times 10^{-5}$).

While no SNPs achieved genome-wide significance, 1 SNP on chromosome 24 approached suggestive significance (chr24:59830666, $P = 1.10 \times 10^{-5}$). Three SNPs, within the same region on chromosome 24, were the next highest associated SNPs (chr24:59876409, $P = 2.77 \times 10^{-5}$; chr24:59940802, $P = 9.40 \times 10^{-5}$; and chr24:60251280, $P = 2.09 \times 10^{-4}$).

Based on the results of genome-wide association analysis, a region of interest was located on chromosome 24 from bp 59,830,666 to 60,251,280. We examined this region, and the surrounding 1 Mb region, for potential candidate genes. Genes in this region included phorbol-12-myristate-13-acetate-induced protein 1 (*PMAIP1*), melanocortin 4 receptor (*MC4R*), glutamate decarboxylase-like 1 (*GADL1*), cadherin-20 (*CDH20*), ring finger protein

152 (*RNF152*), phosphatidylinositol glycan anchor biosynthesis class N (*PIGN*), RAB11 binding and LisH domain, coiled-coil and HEAT repeat containing (*KIAA1468/RELCH*), a member of the tumor necrosis factor receptor family (*TNFRSF11A*, also known as *RANK*), zinc finger CCHC-type containing 2 (*ZCCHC2*), and PH domain and leucine-rich repeat protein phosphatase 1 (*PHLPP1*). In addition, 2 long noncoding RNAs (loc106503556 and loc108633767) are also annotated in the region.

Discussion

This study provided the first detailed clinical and genetic description of a carpal hyperextension syndrome in the NDG breed. Atraumatic carpal hyperextension in this breed, particularly when noted between 3 and 24 months and accompanied by lameness, should prompt evaluation for this condition by clinicians and owners. We propose that goniometry performed in squarely weight-bearing animals is a straightforward and inexpensive diagnostic technique for confirming and characterizing the severity of hyperextension. Normal goats have very straight forelimbs, with nil to very minimal angulation of the carpi on goniometry. In contrast, goats between the ages of 12 and 36 months with carpal angles of 187° or greater should be strongly suspected of having the condition. Affected goats are often lame and may have radiographic signs of degenerative joint disease. However, the various imaging techniques described in this study as well as extensive necropsy evaluation were unable to identify an etiologic cause or contributing structures. It was unclear whether the gross and histopathologic changes in articular and periarticular tissues described in this report were a cause or consequence of the underlying disorder; however, we speculate that carpal hyperextension may reflect a primary problem of idiopathic joint instability leading to the development of secondary degenerative changes. Although a larger proportion of affected goats were bucks, both sexes were commonly affected and we could not distinguish an effect of sex from an effect of the source populations used for sampling.

Similar forelimb hyperextension conditions have been reported in dogs and llamas.¹⁵⁻¹⁸ Canine carpal hyperextension appears to be largely related to trauma¹⁵ though may be degenerative in some breeds or spontaneous in skeletally immature dogs.¹⁶ A series of studies^{17,18} of metacarpophalangeal and metatarsophalangeal hyperextension in llamas found that affected llamas had higher serum zinc and molybdenum and lower liver copper and cobalt concentrations as compared to controls. In the current study, we did not detect any management or nutritional factors associated specifically with the occurrence of carpal hyperextension in goats and found no difference in a wide range of serum mineral concentrations between cases and controls.

Pedigree analysis suggested that all hyperextension cases included in this study shared a single common ancestor, lending support to owner reports of a familial association. We were struck by parallels between this syndrome in goats and inherited joint hypermobility syndromes of humans.¹⁹ Human joint hypermobility often co-occurs with a set of connective tissue disorders grouped as

Ehlers-Danlos syndrome (EDS; comprised of 13 subtypes), with classic EDSs associated with concomitant skin and/or other connective tissue pathologies. Genes underlying classic EDS subtypes in humans are well-defined, with the greatest proportion of affected individuals carrying mutations in structural collagen genes, collagen-processing proteins, or extracellular matrix proteins.¹⁹ No genes underlying human classic EDS map to chromosome 24 of goats. In contrast to classic EDS, human hypermobile EDS (hEDS) is a heritable condition with a female sex predilection and primarily causes joint laxity with concomitant musculoskeletal complications, along with minor skin signs. This disorder has not yet been genetically defined.^{19,20} Hypermobile EDS has a large degree of phenotypic overlap with hypermobility spectrum disorder (HSD), which is a diagnosis of exclusion for cases that do not fully meet hEDS diagnostic criteria.²¹ Both disorders are characterized by disruption of fibroblasts' extracellular matrix and cellular cytostructure and now thought to represent a disease spectrum, rather than 2 distinct conditions.^{22,23} Cultured hEDS and HSD cells have altered transcriptome patterns of many cellular adhesion molecules, namely cadherins and protocadherins (along with desmosomal proteins and claudins), as well as altered proteome profiles.^{24,25} Thus, we found it interesting that 3 classical type II cadherins (*CDH7*, *CDH19*, *CDH20*) map to goat chromosome 24, including 1 (*CDH20*) to the region of interest. Type II cadherins are poorly understood, as compared to type I classical cadherins, yet are known to play crucial role in organizing extracellular matrix, cell-cell interactions, and connective tissue development via interactions with β -catenin in cellular adherens junctions.^{26,27} Cadherin-20 is linked to homologous genes cadherin-7 (*CDH7*) and cadherin-19 (*CDH19*) on human chromosome 18. All 3 are homologous to chicken cadherin-7, which is crucial for limb bud chondrogenesis.^{28,29} In the mouse (*Mus musculus*) and human, *CDH20* is maximally expressed in CNS tissue; however, it is also expressed in a variety of other tissues, including the heart, alimentary structures, and the limb. Tissue specificity of *CDH20* expression in mice is dependent on genetic background, with the degree of expression within somite mesoderm dependent on mouse strain.³⁰ These strain-dependent differences in cell and tissue specificity could relate to variability affinity in forming heterodimers with other type II family members.²⁷ Given the role of cadherins in development, as well as perturbed cadherin transcriptomes in cultured hEDS and HSD cells, further evaluation of *CDH20* may be warranted in goats with carpal hyperextension.

PMAIP1, *MC4R*, *PIGN*, *KIAA1468*, *TNFRSF11A*, and *ZCCHC2* were all additional genes located within the region of interest. These genes have been identified in shared haplotypes of human patients with rheumatoid arthritis.³¹ *PMAIP1* encodes the protein NOXA, which plays an important role in apoptosis, and *PMAIP1* may also represent a risk factor for osteoporosis via the suppression of autophagy in osteoblasts.³² *MC4R* is a melanocortin receptor expressed in the brain, mutations of which are often associated with early-onset obesity in both human and animal models.^{33,34} *PIGN*'s enzyme product participates in the synthesis of glycosylphosphatidylinositol-anchored proteins. Although a number of neurologic disorders have been linked to *PIGN* variant alleles, none affecting musculoskeletal function

have been reported.³⁵ *KIAA1468*, now known as *RELCH*, encodes an intracellular cholesterol transporter,³⁶ which has a possible association with carcass composition in swine.³⁷ *TNFRSF11A* encodes RANK protein, a member of the tumor necrosis factor superfamily that regulates osteoclast activity. Reported mutations primarily manifest as excessive bone deposition (osteopetrosis) or increased bone turnover (Paget disease and related disorders).³⁸ Genetic variants in *TNFRSF11A* may also be associated with increased severity in rheumatoid arthritis.³⁹ Finally, *ZCCHC2* is a tumor suppressor gene associated with retinoblastoma.⁴⁰ While several of these genes may not necessarily fit within the clinical presentation of carpal hyperextension, it is interesting that this combination of genes is notably associated with rheumatoid arthritis in humans.³¹

Other protein-encoding genes found in the region of suggestive SNP association have less plausible relationships with a disorder of joint hypermobility. *RNF152* is one of a large family of ubiquitin ligases that have been implicated in carcinogenesis, but not musculoskeletal disorders. *GADL1* plays an important role in the decarboxylation of amino acids that are essential to skeletal muscle function and additionally contributes to carcass quality in beef cows.⁴¹ A *GADL1* knockout mouse model exhibited stunted growth, decreased tissue levels of amino acids, and elevated markers of oxidative stress.⁴²

Results from our genome-wide association analysis were quite preliminary due to the relatively small sample size and high sampling bias towards females in our overall study population. Analysis of additional case and control animals must be undertaken to robustly identify any SNPs associated with carpal hyperextension. Whole genome sequencing could subsequently identify putative genetic variants between cases and controls. Additionally, we have not yet characterized carpal hyperextension syndrome at a cellular biology or ultrastructural level. Transmission electron microscopy of dermal and musculoskeletal connective tissue can show abnormal collagen fibrils in a large proportion of human hEDS. In addition, ultrastructural characterization of additional components of extracellular matrix in cases may aid in defining underlying pathophysiology.⁴³ On a molecular level, proteome/transcriptome analysis from cultured fibroblasts of affected and unaffected animals would also aid in characterizing perturbations in cellular adhesion molecules.

Currently, it is not known whether any treatment could prevent development of carpal hyperextension or delay its progression. There is currently no evidence-based directed treatment for human hEDS/HDS; preliminary work in cell culture suggests that inhibition of matrix metalloproteinases may delay extracellular matrix disruption.⁴⁴ Analgesic medications may be used to control lameness and improve welfare of affected goats. We do not recommend breeding affected animals due to the possibility of heritability suggested by our results.

Acknowledgments

The authors acknowledge Ashley Richardson and Kate Ness.

Disclosures

Dr. White is an Associate Editor for *JAVMA* and was not involved in the editorial evaluation of or decision to accept this article for publication.

No AI-assisted technologies were used in the composition of this manuscript.

Funding

This study was funded by owners and other individuals through a university fundraising platform.

ORCID

Christiane Löhner  <https://orcid.org/0000-0003-3787-5583>

References

- Cooper T. Breed profile: Nigerian Dwarf goat. How long do Nigerian Dwarf goats live? ... And other breed facts. *Goat Journal*. February 16, 2022. Accessed July 15, 2025. <https://goatjournal.iamcountryside.com/goat-breeds/all-about-nigerian-dwarf-goats/>
- Valencia-Posadas M, Lechuga-Arana AA, Ávila-Ramos F, Shepard L, Montaldo HH. Genetic parameters for somatic cell score, milk yield and type traits in Nigerian Dwarf goats. *Anim Biosci*. 2022;35(3):377-384. doi:10.5713/ab.21.0143
- American Dairy Goat Association. Annual reports. American Dairy Goat Association. Accessed July 15, 2025. <https://adga.org/annual-report/>
- Carpal Hyperextension in Nigerian Dwarf Goats Facebook page. Accessed December 13, 2025. <https://www.facebook.com/groups/320584909045198/>
- Villaquiran M, Gipson TA, Merkel RC, Goetsch AL, Sahl T. Body condition scores in goats. Langston University. Accessed October 12, 2025. https://www.in.gov/boah/files/Goats_BCS_pamphlet.pdf
- Sprecher DJ, Hostetler DE, Kaneene JB. A lameness scoring system that uses posture and gait to predict dairy cattle reproductive performance. *Theriogenology*. 1997;47(6):1179-1187. doi:10.1016/S0093-691X(97)00098-8
- Jaegger G, Marcellin-Little DJ, Levine D. Reliability of goniometry in Labrador Retrievers. *Am J Vet Res*. 2002;63(7):979-986. doi:10.2460/ajvr.2002.63.979
- Formenton MR, de Lima LG, Vassalo FG, Joaquim JGF, Rosseto LP, Fantoni DT. Goniometric assessment in French Bulldogs. *Front Vet Sci*. 2019;6:424. doi:10.3389/fvets.2019.00424
- ADGA Genetics. American Dairy Goat Association, Council on Dairy Cattle Breeding, and Gene Dershowitz. Accessed October 28, 2025. <https://genetics.adga.org/>
- Pedigree Online. Select Web Ventures LLC. Accessed November 9, 2025. <https://www.allbreedpedigree.com/>
- Garbe JR, Da Y. *Pedigree: A Software Tool for the Graphing and Analysis of Large Complex Pedigree*. Version 2.4. University of Minnesota Department of Animal Science; 2008. Accessed July 16, 2025. <https://conservancy.umn.edu/server/api/core/bitstreams/d684e7ba-0b26-4d52-bea2-2fd6c3f36c4a/content>
- Purcell S, Neale B, Todd-Brown K, et al. PLINK: a tool set for whole-genome association and population-based linkage analyses. *Am J Hum Genet*. 2007;81(3):559-575. doi:10.1086/519795
- Turner SD. qqman: an R package for visualizing GWAS results using Q-Q and Manhattan plots. *J Open Source Softw*. 2018;3(25):731. doi:10.21105/joss.00731
- Vuckovic D, Gasparini P, Soranzo N, Iotchkova V. MultiMeta: an R package for meta-analyzing multi-phenotype genome-wide association studies. *Bioinformatics*. 2015;31(16):2754-2756. doi:10.1093/bioinformatics/btv222
- Beierer LH. Canine carpal injuries: from fractures to hyperextension injuries. *Vet Clin North Am Small Anim Pract*. 2021;51(2):285-303. doi:10.1016/j.cvs.2020.12.002
- Whitelock R. Conditions of the carpus in the dog. *In Pract*. 2001;23(1):2-13. doi:10.1136/inpract.23.1.2
- Reed SK, Semevolos SA, Rist PK, Valentine BA. Morphologic and biochemical characterization of hyperextension of the metacarpophalangeal and metatarsophalangeal joints in llamas. *Am J Vet Res*. 2007;68(8):879-885. doi:10.2460/ajvr.68.8.879
- Semevolos SA, Reed SK. Molecular, histologic, and trace mineral characterization of metacarpophalangeal and metatarsophalangeal joint hyperextension in juvenile llamas. *Am J Vet Res*. 2011;72(4):550-555. doi:10.2460/ajvr.72.4.550
- Malfait F, Wenstrup RJ, De Paepe A. Clinical and genetic aspects of Ehlers-Danlos syndrome, classic type. *Genet Med*. 2010;12(10):597-605. doi:10.1097/GIM.0b013e3181eed412
- Castori M, Dordoni C, Valiante M, et al. Nosology and inheritance pattern(s) of joint hypermobility syndrome and Ehlers-Danlos syndrome, hypermobility type: a study of intrafamilial and interfamilial variability in 23 Italian pedigrees. *Am J Med Genet A*. 2014;164A(12):3010-3020. doi:10.1002/ajmg.a.36805
- Castori M, Tinkle B, Levy H, Grahame R, Malfait F, Hakim A. A framework for the classification of joint hypermobility and related conditions. *Am J Med Genet C Semin Med Genet*. 2017;175(1):148-157. doi:10.1002/ajmg.c.31539
- Wang TJ, Stecco A, Hakim AJ, Schleip R. Fascial pathophysiology in hypermobility spectrum disorders and hypermobile Ehlers-Danlos syndrome: a review of emerging evidence. *Int J Mol Sci*. 2025;26(12):5587. doi:10.3390/ijms26125587
- Zoppi N, Chiarelli N, Binetti S, Ritelli M, Colombi M. Dermal fibroblast-to-myofibroblast transition sustained by $\alpha\text{v}\beta\text{3}$ integrin-ILK-Snail1/Slug signaling is a common feature for hypermobile Ehlers-Danlos syndrome and hypermobility spectrum disorders. *Biochim Biophys Acta Mol Basis Dis*. 2018;1864(4)(4 Pt A):1010-1023. doi:10.1016/j.bbadis.2018.01.005
- Chiarelli N, Ritelli M, Zoppi N, Colombi M. Cellular and molecular mechanisms in the pathogenesis of classical, vascular, and hypermobile Ehlers-Danlos syndromes. *Genes (Basel)*. 2019;10(8):609. doi:10.3390/genes10080609
- Chiarelli N, Zoppi N, Ritelli M, et al. Biological insights in the pathogenesis of hypermobile Ehlers-Danlos syndrome from proteome profiling of patients' dermal myofibroblasts. *Biochim Biophys Acta Mol Basis Dis*. 2021;1867(4):166051. doi:10.1016/j.bbadis.2020.166051
- Yulis M, Kusters DHM, Nusrat A. Cadherins: cellular adhesive molecules serving as signalling mediators. *J Physiol*. 2018;596(17):3883-3898. doi:10.1113/JP275328
- Brasch J, Katsamba PS, Harrison OJ, et al. Homophilic and heterophilic interactions of type II cadherins identify specificity groups underlying cell-adhesive behavior. *Cell Rep*. 2018;23(6):1840-1852. doi:10.1016/j.celrep.2018.04.012
- Kools P, Van Imschoot G, van Roy F. Characterization of three novel human cadherin genes (*CDH7*, *CDH19*, and *CDH20*) clustered on chromosome 18q22-q23 and with high homology to chicken cadherin-7. *Genomics*. 2000;68(3):283-295. doi:10.1006/geno.2000.6305
- Kim D, Kang SS, Jin EJ. Alterations in the temporal expression and function of cadherin-7 inhibit cell migration and condensation during chondrogenesis of chick limb mesenchymal cells in vitro. *J Cell Physiol*. 2009;221(1):161-170. doi:10.1002/jcp.21840. Published correction appears in *J Cell Physiol*. 2020;235(5):4982. doi:10.1002/jcp.29406
- Moore R, Champeval D, Denat L, et al. Involvement of cadherins 7 and 20 in mouse embryogenesis and melanocyte transformation. *Oncogene*. 2004;23(40):6726-6735. doi:10.1038/sj.onc.1207675
- Ziegler A, Ewhida A, Brendel M, Kleensang A. More powerful haplotype sharing by accounting for the mode

- of inheritance. *Genet Epidemiol.* 2009;33(3):228–236. doi:10.1002/gepi.20373
32. Gao Y, Huang A, Zhao Y, Du Y. PMAIP1 regulates autophagy in osteoblasts via the AMPK/mTOR pathway in osteoporosis. *Hum Cell.* 2024;37(4):1024–1038. doi:10.1007/s13577-024-01067-w
 33. Loos RJ, Lindgren CM, Li S, et al; Prostate, Lung, Colorectal, and Ovarian Cancer Screening Trial; KORA; Nurses' Health Study; Diabetes Genetics Initiative; SardiNIA Study; Wellcome Trust Case Control Consortium; FUSION. Common variants near *MC4R* are associated with fat mass, weight and risk of obesity. *Nat Genet.* 2008;40(6):768–775. doi:10.1038/ng.140
 34. Huszar D, Lynch CA, Fairchild-Huntress V, et al. Targeted disruption of the melanocortin-4 receptor results in obesity in mice. *Cell.* 1997;88(1):131–141. doi:10.1016/S0092-8674(00)81865-6
 35. Loong L, Tardivo A, Knaus A, et al. Biallelic variants in *PIGN* cause Fryns syndrome, multiple congenital anomalies-hypotonia-seizures syndrome, and neurologic phenotypes: A genotype-phenotype correlation study. *Genet Med.* 2023;25(1):37–48. doi:10.1016/j.gim.2022.09.007
 36. Sobajima T, Yoshimura SI, Maeda T, Miyata H, Miyoshi E, Harada A. The Rab11-binding protein RELCH/KIAA1468 controls intracellular cholesterol distribution. *J Cell Biol.* 2018;217(5):1777–1796. doi:10.1083/jcb.201709123
 37. Heidaritabar M, Bink MCAM, Dervishi E, Charagu P, Huisman A, Plastow GS. Genome-wide association studies for additive and dominance effects for body composition traits in commercial crossbred Piétrain pigs. *J Anim Breed Genet.* 2023;140(4):413–430. doi:10.1111/jbg.12768
 38. Xue JY, Ikegawa S, Guo L. Genetic disorders associated with the RANKL/OPG/RANK pathway. *J Bone Miner Metab.* 2021;39(1):45–53. doi:10.1007/s00774-020-01148-4
 39. Triguero-Martínez A, Pardines M, Montes N, et al. Genetic variants in RANK and OPG could influence disease severity and bone remodeling in patients with early arthritis. *Life (Basel).* 2024;14(9):1109. doi:10.3390/life14091109
 40. Wang Y, Yu Y, Pang Y, et al. The distinct roles of zinc finger CCHC-type (ZCCHC) superfamily proteins in the regulation of RNA metabolism. *RNA Biol.* 2021;18(12):2107–2126. doi:10.1080/15476286.2021.1909320
 41. Li Y, Wang M, Li Q, et al. Transcriptome profiling of longissimus lumborum in Holstein bulls and steers with different beef qualities. *PLoS One.* 2020;15(6):e0235218. doi:10.1371/journal.pone.0235218
 42. Mahootchi E, Cannon Homaei S, Kleppe R, et al. *GADL1* is a multifunctional decarboxylase with tissue-specific roles in β -alanine and carnosine production. *Sci Adv.* 2020;6(29):eabb3713. doi:10.1126/sciadv.abb3713
 43. Gensemer C, Burks R, Kautz S, Judge DP, Lavallee M, Norris RA. Hypermobile Ehlers-Danlos syndromes: complex phenotypes, challenging diagnoses, and poorly understood causes. *Dev Dyn.* 2021;250(3):318–344. doi:10.1002/dvdy.220
 44. Chiarelli N, Zoppi N, Venturini M, et al. Matrix metalloproteinases inhibition by doxycycline rescues extracellular matrix organization and partly reverts myofibroblast differentiation in hypermobile Ehlers-Danlos syndrome dermal fibroblasts: a potential therapeutic target? *Cells.* 2021;10(11):3236. doi:10.3390/cells10113236

Supplementary Materials

Supplementary materials are posted online at the journal website: avmajournals.avma.org.